Evidence for Myocardial ATP Compartmentation from NMR Inversion Transfer Analysis of Creatine Kinase Fluxes

F. Joubert,* B. Gillet,† J. L. Mazet,* P. Mateo,* J.-C. Beloeil,† and J. A. Hoerter*

*Institut National de la Santé et de la Recherche Médicale U-446, Laboratory of Cellular and Molecular Cardiology, Université Paris-Sud, Chatenay Malabry, and †Résonance Magnétique Nucléaire Biologique, ICSN, Centre National de la Recherche Scientifique, Gif-sur-Yvette, France

ABSTRACT The interpretation of creatine kinase (CK) flux measured by ^{31}P NMR magnetization transfer in vivo is complex because of the presence of competing reactions, metabolite compartmentation, and CK isozyme localization. In the isovolumic perfused rat heart, we considered the influence of both ATP compartmentation and ATP-P_i exchange on the forward (F_f: PCr $\rightarrow$ ATP) and reverse (F_r) CK fluxes derived from complete analysis of inversion transfer. Although F_f should equal F_r because of the steady state, in both protocols when PCr (inv-PCr) or ATP (inv-ATP) was inverted and the contribution of ATP-P_i was masked by saturation of P_i (sat-P_i), F_f/F_r significantly differed from 1 (0.80 $\pm$ 0.06 or 1.32 $\pm$ 0.06, respectively, $n = 5$). These discrepancies could be explained by a compartment of ATP (f_{ATP}) not involved in CK. Consistently, neglecting ATP compartmentation in the analysis of CK in vitro results in an underestimation of F_f/F_r for inv-PCr and its overestimation for inv-ATP. Both protocols gave access to f_{ATP} if the system was adequately analyzed. The fraction of ATP not involved in CK reaction in a heart performing medium work amounts to 20–33% of cellular ATP. Finally, the data suggest that the effect of sat-P_i might not result only from the masking of ATP-P_i exchange.

INTRODUCTION

The creatine kinase (CK) catalyzes the reversible exchange of high-energy phosphate:

$$PCr^{2-} + MgADP^{-} + H^{+} \rightleftarrows Cr + MgATP^{2-}$$

Despite considerable efforts devoted to the study of the flux of this enzyme by ^{31}P NMR spectroscopy, there is still some controversy about the equivalence of the various magnetization transfer techniques and about the physiological interpretation of the NMR measured CK fluxes. The development of transgenic mice with specific CK isoform knockout has renewed the interest in the analysis of CK flux (Van Dorsten et al., 1998).

The role of different CK isoforms in the myocardium is still under debate: a cytosolic CK working close to equilibrium might account for the replenishment of ATP stores upon ATP utilization and the energy diffusion across the cell. On the other hand, bound CK specifically localized close to sites of energy production and utilization might play a major role in myocardial energy transduction. Nevertheless, even if the bound isoforms have kinetics different from those of the cytosolic CK, the cell is in steady state, and PCr is only metabolized by CK. Therefore, both total CK fluxes (corresponding to the unidirectional flux of production and consumption of ATP by CK) measured by NMR should be equal.

The main problem in the interpretation of a magnetization transfer experiment in vivo arises from the oversimplification of a highly organized cellular system: in other words, the interpretation of data is always model dependent. Most of the work devoted to cardiac CK flux has been performed by saturation transfer technique (ST). Consistent data have been obtained for the determination of the forward CK flux PCr $\rightarrow$ ATP (F_f), whereas a large range of values has been reported in the literature for the reverse CK flux ATP $\rightarrow$ PCr (F_r) (see Table 1). When a discrepancy between F_f and F_r was observed, two main alternative hypotheses were proposed. First, the two-site model of CK reaction has been recognized as an oversimplification of the system: ATP is involved in other exchanges, mainly with P_i (Ugurbil et al., 1986; Spencer et al., 1988), but also with glycolytic metabolites (Matthews et al., 1982; Brindle, 1988). The second hypothesis is the presence of an ATP compartmentation initially suggested by Nunnally and Hollis (1979). The discrepancy between fluxes, which increases with cardiac performance (Koretsky et al., 1985), was further proposed to result from the presence of an additional exchange between either PCr and a small NMR-visible ATP pool (Korestky et al., 1985, 1986) or between PCr and a nonvisible nonsaturated ATP compartment (Zahler et al., 1987; Zahler and Ingwall, 1992).

Inversion transfer (IT) has mainly been performed in muscle by analyzing the initial rate of recovery, which allowed a simplification of the mathematical analysis and a reduction in experimental time (Hsieh and Balaban, 1988; McFarland et al., 1994). However, the complete analysis of the evolution of the magnetization of the inverted and noninverted species permits the determination in the same experiment of both F_f and F_r (Led and Gesmar, 1982). Furthermore, data can then be analyzed without imposing the equilibrium of CK on the system, while this simplifica-

Received for publication 1 October 1999 and in final form 10 April 2000.

Address reprint requests to Dr. Jacqueline A. Hoerter, U-446 INSERM, Cardiologie Cellulaire et Moleculaire, Faculté de Pharmacie, 5 rue J. B. Clément, 92296 Chatenay-Malabry, France. Tel.: 33-1-46835759; Fax: 33-1-46835475; E-mail: jacqueline.hoerter@cep.u-psud.fr.

0006-3495/00/07/01/13 $2.00

TABLE 1 Comparison of published values of the F_f/F_r ratio

Experiment	Substrate	Organ	F_f/F_r	Reference
Saturation				
SSST	Acetate*	Heart	2.1	Matthews et al. (1982)
	Pyruvate†	Heart	1.8	Ugurbil et al. (1986)
	Pyruvate	Heart	3.0	Zweier and Jacobus (1987)
	Glucose*	Heart	1.2	Matthews et al. (1982)
	Glucose	Heart	1.0	Degani et al. (1985)
	Glucose	Heart	1.1	Ugurbil et al. (1986)
	Glucose	Heart	1.2	Zweier and Jacobus (1987)
	In vivo	Heart	1.6	Koretsky et al. (1986)
	In vivo	Skeletal muscle	2.0	Hsieh and Balaban (1988)
TDST	Acetate	Heart	1.6	Nunnally and Hollis (1979)
	Glucose*	Heart	1.4	Bittl and Ingwall (1985)
	Glucose	Heart	1.5	Spencer et al. (1988)
	In vivo	Heart	1.1	Bittl et al. (1987)
	In vivo	Skeletal muscle	1.1	Bittl et al. (1987)
Inversion				
Initial slope	Pyruvate	Skeletal muscle	1.0	McFarland et al. (1994)
	In vivo	Skeletal muscle	0.9	Hsieh and Balaban (1988)
	In vivo	Brain	1.5	Mora et al. (1992)
Full analysis	Glucose	Heart	1.0	Degani et al. (1985)
	In vivo	Brain	1.2	Degani et al. (1987)
	In vivo	Brain	0.6	Mora et al. (1992)

SSST, Steady-state saturation transfer; TDST, time-dependent saturation transfer.
*In the absence of contractile activity F_f/F_r is 1 in both glucose or acetate KCl arrested hearts.
†Both pyruvate and glucose present.
This table emphasizes the influence of various factors on the determination of F_f/F_r: the magnetization transfer protocol, the substrate used, and the work performed.

tion of the Bloch equations is usually applied in the analysis of ST. Such analysis of IT offers a definitive advantage over the other magnetization transfer techniques.

Using IT, we found unequal CK fluxes in myocardium. To interpret these data, we analyzed the consequences for the measured CK fluxes of the presence of an ATP pool not involved in the CK reaction (or in slow exchange), as earlier suggested by Meyer et al. (1982). We considered total cellular ATP and PCr to be fully NMR visible and disturbed by the inversion procedure. The Bloch equations were modified to take into account this additional compartment of ATP, in both cases of an inversion of PCr (inv-PCr) and of γATP (inv-γATP) (see section Theory).

Our aim was to explore the capacity of a full time-course analysis of inversion transfer to reveal experimentally both the specific contributions of ATP compartmentation and ATP-P_i exchange in the CK fluxes of a perfused heart. Based on in vitro simulation we show that the presence of an ATP compartment (not exchanging with PCr) is consistent with the flux discrepancies observed in situ. Moreover, under conditions designed to mask the influence of ATP-P_i exchange, this ATP compartment could be independently quantified in both inv-PCr and inv-γATP protocols.

THEORY

Classical Bloch equations for chemical exchange (McConnell, 1958) had to be modified to account first for the fraction of ATP not involved in the CK reaction, f_{ATP}, and second for the involvement of ATP in other reactions. In the following sections we refer to a phosphorus species as a "site" and a kinetic compartment as a "compartment."

Model I: two-site two-compartment analysis: basic model

The CK reaction is considered as a two-site exchange of the ^{31}P nucleus:

$$\mathrm{PCr} \underset{k_r}{\overset{k_f}{\rightleftarrows}} \gamma\mathrm{ATP} \qquad \text{Model I}$$

where k_f and k_r are, respectively, the forward and reverse pseudo-first-order rate constants of the reaction. Considering the magnetization at equilibrium, M^{∞}_{PCr} and $M^{\infty}_{\gamma ATP}$, the forward flux PCr → ATP and the reverse flux ATP → PCr are given respectively by

$$F_f = k_f \cdot M^{\infty}_{PCr} \tag{1}$$

$$F_r = k_r \cdot M^{\infty}_{\gamma ATP} \tag{2}$$

The evolution of magnetization is described by the modified Bloch equations (Ugurbil, 1985), where $T_{1\gamma ATP}$, T_{1PCr} are the intrinsic relaxation parameters:

$$dM_{PCr}/dt = -(k_f + 1/T_{1PCr})(M_{PCr} - M^{\infty}_{PCr}) + k_r(M_{\gamma ATP} - M^{\infty}_{\gamma ATP}) \tag{3}$$

$$dM_{\gamma ATP}/dt = -(k_r + 1/T_{1\gamma ATP})(M_{\gamma ATP} - M^{\infty}_{\gamma ATP}) + k_f(M_{PCr} - M^{\infty}_{PCr}) \quad (4)$$

The solutions of this system depend on the protocol of magnetic perturbation.

Time-dependent saturation transfer

Upon full saturation of γATP ($M_{\gamma ATP} = 0$), M_{PCr} decreases because of chemical exchange between PCr and γATP. Considering the equilibrium of CK, $k_f \cdot M^{\infty}_{PCr} = k_r \cdot M^{\infty}_{\gamma ATP}$, Eq. 3, which describes the time evolution of M_{PCr} becomes

$$M_{PCr}(t) = M^{ss}_{PCr} + (M^{\infty}_{PCr} - M^{ss}_{PCr})\exp[-(k_f + 1/T_{1PCr})t] \quad (5)$$

where $M^{ss}_{PCr} = M^{\infty}_{PCr}/(1 + k_f T_{1PCr})$. From this experiment k_f and T_{1PCr} may be derived. Forward flux F_f is determined from the accurate knowledge of M^{∞}_{PCr} and Eq. 1.

Inversion transfer

After a selective inversion of either PCr or γATP, the chemical exchange occurs between the two magnetizations. In this case, the solutions of Eq. 3 and 4 are given by the general expression (Led and Gesmar, 1982):

$$M_{PCr}(t) = M^{\infty}_{PCr} + C_1\exp\lambda_1 t + C_2\exp\lambda_2 t \quad (6)$$

$$M_{\gamma ATP}(t) = M^{\infty}_{\gamma ATP} + C_3\exp\lambda_1 t + C_4\exp\lambda_2 t \quad (7)$$

with

$$\lambda_1 = 1/2\{-(k_{1f} + k_{1r}) + [(k_{1f} - k_{1r})^2 + 4k_f k_r]^{1/2}\}$$

$$\lambda_2 = 1/2\{-(k_{1f} + k_{1r}) - [(k_{1f} - k_{1r})^2 + 4k_f k_r]^{1/2}\}$$

where

$$k_{1f} = k_f + 1/T_{1PCr} \quad k_{1r} = k_r + 1/T_{1\gamma ATP}$$

and

$$C_1 = \{(\lambda_2 + k_{1f})(M^{\infty}_{PCr} - M_{PCr}(0)) - k_r(M^{\infty}_{\gamma ATP} - M_{\gamma ATP}(0))\}/(\lambda_1 - \lambda_2)$$

$$C_2 = \{-(\lambda_1 + k_{1f})(M^{\infty}_{PCr} - M_{PCr}(0)) + k_r(M^{\infty}_{\gamma ATP} - M_{\gamma ATP}(0))\}/(\lambda_1 - \lambda_2)$$

$$C_3 = \{-k_f(M^{\infty}_{PCr} - M_{PCr}(0)) - (\lambda_1 + k_{1f}) \cdot (M^{\infty}_{\gamma ATP} - M_{\gamma ATP}(0))\}/(\lambda_1 - \lambda_2)$$

$$C_4 = \{k_f(M^{\infty}_{PCr} - M_{PCr}(0)) + (\lambda_2 + k_{1f}) \cdot (M^{\infty}_{\gamma ATP} - M_{\gamma ATP}(0))\}/(\lambda_1 - \lambda_2)$$

From inversion of PCr, or of γATP, the four parameters of the reaction, k_f, k_r, T_{1PCr}, $T_{1\gamma ATP}$ may be computed independently, and both F_f and F_r fluxes calculated from Eqs. 1. and 2.

Model II: two-site three-compartment analysis: modification accounting for a compartment of ATP not involved in CK

$$PCr \underset{k_r}{\overset{k_f}{\rightleftarrows}} \gamma ATP_1 \quad \gamma ATP_2 \qquad \text{Model II}$$

In the case of two pools of ATP, one pool, $ATP_1 = (1 - f_{ATP}) \cdot ATP$, in fast exchange with PCr, and a second, $ATP_2 = f_{ATP} \cdot ATP$, not exchanging (or in slow exchange) with PCr, the evolution of each pools must be considered separately; the time evolution of ATP_1 is described by Eq. 4, and that of ATP_2 by

$$dM_{\gamma ATP_2}/dt = -(M_{\gamma ATP_2} - M^{\infty}_{\gamma ATP_2})/T_{1\gamma ATP_2} \quad (8)$$

The solutions of this new system (Eqs. 3, 4, and 8) depend on the type of magnetization transfer protocol. In time-dependent saturation transfer (TDST), neglecting ATP compartmentation will not affect F_f (measured by saturation of γATP). F_r, measured by saturation of PCr, will also be correct, as pointed out earlier (Meyer et al., 1982; Spencer et al., 1988): the underestimation of k_r (by $1 - f_{ATP}$) is indeed exactly compensated for by an overestimation of the ATP content. However, in IT, the presence of an ATP compartment will affect the analysis of both PCr and γATP inversion in a different way.

Inversion of PCr

Magnetization of ATP_2, not initially disturbed, thus is constant during the experiment: $dM_{\gamma ATP_2}/dt = 0$. The evolution of ATP magnetization, $M_{\gamma ATP}(t)$, depends only on $M_{\gamma ATP1}$ and is still described by Eq. 7; that of PCr, $M_{PCr}(t)$, follows Eq. 6. F_f is still given by Eq. 1. However, because only the sum $M_{\gamma ATP} = M_{\gamma ATP1} + M_{\gamma ATP2}$ is experimentally observed, only an apparent reverse flux ($k_r \cdot M^{\infty}_{\gamma ATP}$) is accessible. The steady state is described by $k_f \cdot M^{\infty}_{PCr} = k_r \cdot M^{\infty}_{\gamma ATP_1}$. Because $M^{\infty}_{\gamma ATP} = M^{\infty}_{\gamma ATP_1}/(1 - f_{ATP})$, the ratio F_f/F_r equals $(1 - f_{ATP})$. Therefore, in an inv-PCr protocol, correct kinetic parameters can be obtained, and the measured F_f/F_r directly quantifies the fraction of ATP not involved in the CK reaction.

Inversion of γATP

In this protocol, both γATP_1 and γATP_2 are inverted: $M_{PCr}(t)$ and $M_{\gamma ATP1}(t)$ are still described by Eqs. 6 and 7, but the evolution of $M_{\gamma ATP}$ must now include the evolution of $M_{\gamma ATP_2}$, described by

$$M_{\gamma ATP_2}(t) = M^{\infty}_{\gamma ATP_2} + (M_{\gamma ATP_2}(0) - M^{\infty}_{\gamma ATP_2})\exp[-t/T_{1\gamma ATP_2}] \quad (9)$$

The time evolution of $M_{\gamma ATP}$ is thus described by a triple exponential:

$$M_{\gamma ATP}(t) = M^{\infty}_{\gamma ATP} + C_3 \exp\lambda_1 t + C_4 \exp\lambda_2 t + (M_{\gamma ATP_2}(0) - M^{\infty}_{\gamma ATP_2})\exp - (t/T_{1\gamma ATP_2}) \quad (10)$$

The parameters of the CK reaction, as well as $T_{1\gamma ATP2}$, can be obtained by fitting $M_{\gamma ATP}(t)$ by Eq. 10 and $M_{PCr}(t)$ by Eq. 6. Again, F_f/F_r gives $(1 - f_{ATP})$. Neglecting the contribution of Eq. 9 and performing a two-site analysis will induce errors in all parameters and thus in both fluxes. Notice that in this case, the ratio F_f/F_r will be overestimated.

Model III: three-site three-compartment analysis: modification accounting for the implication of ATP in other exchanges

In contrast to PCr which is only metabolized by CK in the cell, ATP is involved in many other cellular reactions. Because of the high activity of ATP synthesis and hydrolysis in muscle, the ATP-P_i exchange has been recognized as a possible main source of artifact in the determination of CK flux: a three-site three-compartment exchange model has been proposed (Ugurbil et al., 1986; Spencer et al., 1988):

$$PCr \underset{k_r}{\overset{k_f}{\rightleftarrows}} \gamma ATP \underset{k_{d'}}{\overset{k_d}{\rightleftarrows}} P_i \qquad \text{Model III}$$

In this frame, elimination of the effect of $P_i \rightarrow$ ATP exchange by a continuous saturation of P_i (sat-P_i) will reduce the model to a two-site two-compartment exchange (model I) described by a new set of equations analogous in form to Eqs. 3 and 4 (for a complete description, see Ugurbil, 1985):

$$dM_{PCr}/dt = -(k_f + 1/T_{1PCr})(M_{PCr} - M^{*}_{PCr}) + k_r(M_{\gamma ATP} - M^{*}_{\gamma ATP}) \quad (11)$$

$$dM_{\gamma ATP}/dt = -(k_r + 1/T^{*}_{1\gamma ATP})(M_{\gamma ATP} - M^{*}_{\gamma ATP}) + k_f(M_{PCr} - M^{*}_{PCr}) \quad (12)$$

where M^{*}_{PCr} and $M^{*}_{\gamma ATP}$ are the steady-state magnetization under sat-P_i, and $1/T^{*}_{1\gamma ATP} = k_d + 1/T_{1\gamma ATP}$

Model IV: three-site four-compartment analysis: modification accounting for both ATP compartmentalization and the implication of ATP in other exchanges

In the case of ATP compartmentation,

$$PCr \underset{k_r}{\overset{k_f}{\rightleftarrows}} \gamma ATP_1 \underset{k_{d'}}{\overset{k_d}{\rightleftarrows}} P_i \underset{k_h}{\overset{k_s}{\rightleftarrows}} \gamma ATP_2 \qquad \text{Model IV}$$

A complete description of the system in the absence of P_i saturation is given in the Appendix. With the saturation of P_i this model reduces to model II with modified intrinsic relaxation parameters, if the only consequence of sat-P_i is to mask the influence of the $P_i \rightarrow$ ATP exchange. Equation 12 applies to the evolution of $M_{\gamma ATP1}$. The time evolution of $M_{\gamma ATP2}$ is described as previously by model II and Eq. 8. Notice that the determination of F_f by the saturation of γATP is the only experimental protocol that is not influenced by the presence of a $P_i \leftrightarrow$ ATP exchange and can thus be used as a reference for in vivo flux determination.

In summary, this formalism describes how to take into account the presence of an ATP compartment in the analysis of both inversion of PCr and γATP and shows that both protocols can independently quantify an ATP compartment.

MATERIALS AND METHODS

Enzyme solutions

Measurement of CK flux in vitro was performed using two concentric tubes (OD tube 1 = 8 mm, tube 2 = 20 mm). Both tubes contained solutions, the initial composition of which was (in mM) 10 Cr, 5.7 Mg, 1 dithiothreitol, 0.5 EGTA, 100 HEPES, and 15% D_2O. ATP (5 mM), PCr (10 mM), and rabbit muscle creatine kinase (Boehringer) at a concentration of 800 IU/ml were added to tube 1. Variable concentrations of ATP ranging from 0 to 1.2 mM (corresponding to a fraction of ATP_2 not involved in CK reaction ranging from 0 to 50% of the total ATP) were added to tube 2, which did not contain CK. $T_{1\gamma ATP2}$ stays constant and similar to $T_{1\gamma ATP1}$ in this protocol. The pH of the final solutions was adjusted with acetic acid at 7.1 at 30°C. The flux measurement was performed at 30°C. To evaluate the possibility of measuring $T_{1\gamma ATP2}$ in our in vitro system, a second series of experiments was performed in which tube 2 contained a fixed ATP concentration of 1 mM (corresponding to 45% of the total ATP), but its relaxation properties were modified by replacing H_2O in the solution with various amounts of glycerol (from 15 to 70%) to change the viscosity of the solution.

Isolated perfused rat hearts

Animal experimentation was performed in accordance with the Helsinki Accords for Humane Treatment of Animals during Experimentation. Wistar male rats (350–450 g) were anesthetized with ethyl carbamate (2 g/kg), and hearts were perfused by the Langendorff technique at a constant flow of 13.5 ml·min^{-1} as previously described (Hoerter et al., 1988). Briefly, a latex balloon was inserted into the left ventricle (LV) and inflated with D_2O to isovolumic conditions of work. Mean coronary pressure, LV systolic pressure (LVP), end diastolic pressure (EDP), and heart spontaneous frequency were continuously monitored on a computer (Compaq) via Statham gauges. The rate pressure product (RPP in 10^4·mmHg·beats·min^{-1}) was used as an index of contractility reflecting the energetic demand. The perfusion solution contained (in mM) 124 NaCl, 6 KCl, 1.8 $CaCl_2$, 1 $MgSO_4$, 1.1 mannitol, 10 Na-acetate, and 20 HEPES and was oxygenated with 100% O_2. The pH_o was adjusted to 7.35 at 36.5°C. Hearts were freeze clamped at the end of the experiment to measure their ATP, PCr, and Cr contents (in nmol·mg·/prot.$^{-1}$) (Hoerter et al., 1988). These values were used to calculate the metabolite concentrations during magnetization transfer. CK flux was expressed in mM·s^{-1} (assuming cytosolic H_2O volume = 2.72 μl·mg/prot.$^{-1}$).

NMR

^{31}P NMR spectra were acquired on a Innova Varian with a 9.4-T wide-bore magnet in 8-mm- and 20-mm-diameter tubes for the in vitro analysis and in a 20-mm tube for the heart. We used a pulse angle of 80°, 4 K data point acquisition, a spectral width of 10,000 Hz, an acquisition time of 0.205 s, a repetition time of 10 s, zero filling to 8 K, and line broadening of 20 Hz. For all flux measurements, 32-scan spectra were acquired by blocs of eight scans cycling four times through the whole protocol. For the heart experiment, homogeneity was performed on the heart water, the frequency was locked on D_2O contained in the LV balloon, and the 360° pulse duration was measured on the γATP peak. After 20 min of equilibration, four partially saturated spectra (repetition time 2 s, number of scans 32) were acquired. The stability of the preparation was checked by comparing fully relaxed control spectra (repetition time 10 s) acquired before and after the magnetization transfer experiment; any heart showing more than 10% variation in its metabolite content was discarded. These controls were also used to check the complete recovery of magnetization after 10 s of mixing time during inversion protocols. In four hearts TDST of γATP (Bittl and Ingwall, 1985) was performed as a reference for the determination of forward CK flux. Eight spectra were acquired with a duration of γATP saturation ranging from 0 to 9 s (a 9-s irradiation at mirror frequency was used to test radiation spillover). The delays between pulses were adjusted to achieve a constant rate of recurrence of 10 s in each spectrum. Inversion recovery (IR) was used to measure $T_{1\gamma ATP}$ in vitro (eight spectra, 16 scans, delays ranging from 0 to 10 s). The inversion transfer (IT) experiments were performed with a pulse sequence consisting of a frequency-selective sinc pulse (15 ms, bandwidth 300 Hz), a variable mixing time delay (0.2–10 s), a 80° read pulse, and a fixed 10-s delay to allow full relaxation before the next inversion. Each inversion transfer experiment required 26 spectra in vitro (total time 75 min) and 13 spectra for the heart (total time 75 min). Five hearts were used for each protocol of inversion of PCr (inv-PCr) or γATP (inv-γATP). The effect of a shorter repetition time of 4 s was additionally checked in four hearts (inv-PCr, $n = 2$; inv-γATP, $n = 2$). In 10 other hearts inv-γATP or inv-PCr was performed under continuous saturation of P_i. Although off-resonance effects of a sat-P_i protocol on PCr could not be checked directly by mirror irradiation, we considered as negligible the spillover of P_i saturation because similar irradiation applied at 2.4 ppm from PCr (chemical shift of P_i = 4.86 ppm from PCr) resulted in a ~3% decrease in PCr.

Analysis

In TDST protocols, the exponential decay of γATP magnetization, estimated by peak areas, was analyzed to determine in the same experiment T_{1PCr} and k_f (Bittl and Ingwall, 1985). In IT experiments, the adjustment of experimental data with theoretical expression was performed using either the peak areas or the product of peak amplitudes by α, as described by Led and Gesmar (1982), which should address the total NMR visible cellular metabolites. α, the average ratio of peak area to amplitude, was measured for each heart (mean value 0.61 ± 0.02 and 1.50 ± 0.03, $n = 10$, for inv-PCr and inv-γATP, respectively). The two analyses gave similar results; only the latter is shown here because it results in smaller data scattering. The evolution of the inverted and noninverted species was fitted to the solutions of Bloch equations, using the Levenberg-Marquardt method. Equations 6 and 7 were used for the two-site two-compartment analysis of inv-PCr and inv-γATP protocol. The adjustable parameters in this analysis were k_f, k_{1f}, k_r, k_{1r}, and the magnetizations of PCr and ATP at $t = 0$ and $t = \infty$. Two-site three-compartment analysis of the inv-ATP experiment under saturation of P_i had to be performed by a three-exponential fit of $M_{\gamma ATP}$ using Eq. 10. However, because of the number of unknown parameters, the confidence interval for the parameters derived from this analysis was high both in vitro and in the myocardium. To improve this analysis, F_f and T_{1PCr} measured in the inv-PCr experiment were imposed as fixed parameters (for justification see the Results).

All data were expressed as mean ± SE. Differences between groups were analyzed by *t*-test, paired *t*-test, or variance analysis and Student-Newman-Keuls test.

RESULTS

In vitro validation of the model

Variation of fraction of the ATP (f_{ATP}) that does not participate in the CK reaction

To test the model in vitro, the fraction f_{ATP} of ATP not involved in the CK reaction was first varied from 0 to 0.5, while $T_{1\gamma ATP2}$ was kept constant (and equal to $T_{1\gamma ATP1}$).

Inversion of PCr. The parameters of the CK reaction k_f, k_r, T_{1PCr}, and $T_{1\gamma ATP1}$ were first measured in the absence of compartmentalization ($f_{ATP} = 0$). As expected from the in vitro CK kinetics, F_f was equal to F_r. With the increase in f_{ATP}, the values of k_f, k_r, T_{1PCr}, and $T_{1\gamma ATP1}$ remained constant as predicted by the theoretical development; their mean values were $k_f = 0.30 \pm 0.01\ s^{-1}$, $k_r = 0.57 \pm 0.02\ s^{-1}$, $T_{1PCr} = 4.2 \pm 0.3$ s, and $T_{1\gamma ATP1} = 2.4 \pm 0.2$ s. Fig. 1 *a* shows the evolution of the measured F_f and F_r as a function of f_{ATP} as well as their theoretical prediction. The F_f value remained constant ($1.00 \pm 0.04\ MU{\cdot}s^{-1}$). The observed increase in F_r (from 0.98 to 1.96 $MU{\cdot}s^{-1}$) was due solely to the overestimation of the ATP used in the flux calculation. As a result, the ratio F_f/F_r decreased from 1 to 0.5. F_f/F_r was a direct measure of $(1 - f_{ATP})$ as expected from the theory. Indeed, an excellent correlation was observed between the size of the ATP compartment imposed experimentally and its value as estimated by inv-PCr ($r^2 = 0.97$).

Inversion γATP protocol. Likewise, in the absence of ATP compartmentation ($f_{ATP} = 0$), F_f and F_r were equal. When f_{ATP} increased, the two-site three-compartment analysis correctly estimated k_r ($0.56 \pm 0.04\ s^{-1}$), $T_{1\gamma ATP1}$ (2.6 ± 0.4 s), and $T_{1\gamma ATP2}$ (2.5 ± 0.5 s). The fraction f_{ATP} extracted from this analysis was well correlated with the size of the ATP compartment ($r^2 = 0.96$; not shown). Neglecting ATP compartmentation (i.e., analyzing the data by the two-site two-compartment model I) did not allow a correct determination of the rate constants. As the fraction of ATP increased (Fig. 1 *b*), a rise was observed both in k_f (from $0.28\ s^{-1}$ to $0.73\ s^{-1}$) and in F_f (from 1 to 1.77 $MU{\cdot}s^{-1}$). The rate constant k_r decreased from $0.62\ s^{-1}$ to $0.26\ s^{-1}$. One should notice that in this analysis, no significant change could be experimentally detected in F_r (mean $F_r = 0.98 \pm 0.07\ MU{\cdot}s^{-1}$). This result suggests that the error made by neglecting f_{ATP} in the analysis was balanced by an underestimation of k_r: i.e., the error in k_r can be roughly estimated as $(1 - f_{ATP})$. The ratio F_f/F_r increased from 1 to 1.87 $MU{\cdot}s^{-1}$. Again, Scheme II was adequate to predict the measured F_f and F_r in inv-γATP. No change were found in the values of T_{1PCr} and $T_{1\gamma ATP1}$ (3.9 ± 0.4 s and 2.4 ± 0.2 s, respectively). Thus, in the case of ATP

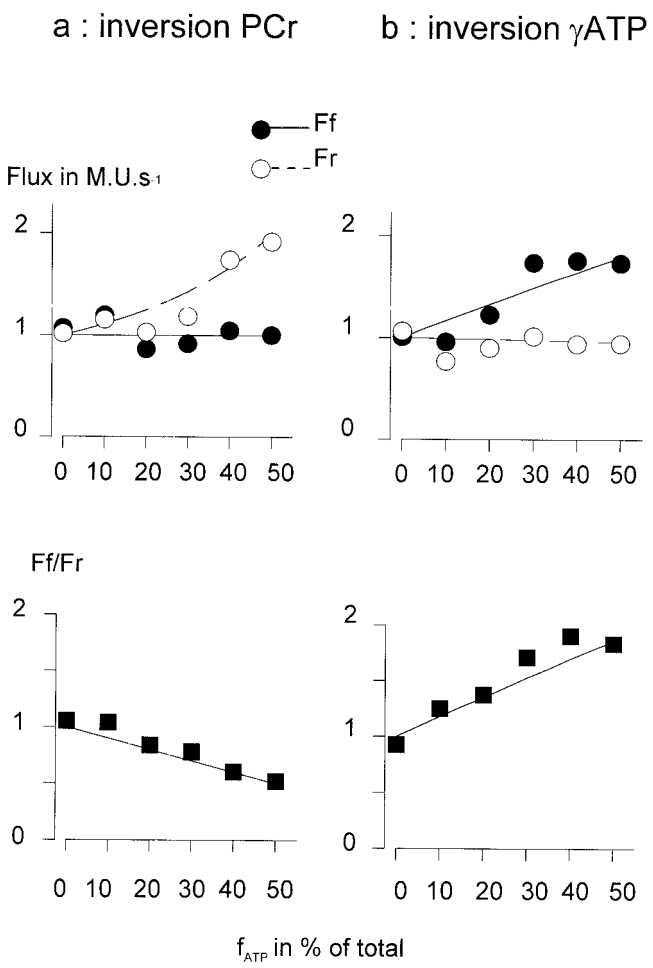

FIGURE 1 Influence of the presence of an ATP compartment on the in vitro determination of CK flux parameters by inversion transfer protocols. (*a*) Protocol of inversion of PCr. (*b*) Protocol of inversion of γATP. Forward and reverse flux (*top*) as well as F_f/F_r ratio (*bottom*) were expressed as a function of ATP_2 (as a percentage of total ATP) when the fraction of ATP not involved in CK (in $tube_2$) was increased. Fluxes (shown in *symbols*) were computed by fitting experimental data to Eqs. 6 and 7. The continuous lines were obtained by fitting Eqs. 6 and 7 to kinetics reconstructed from the known fraction f in Eqs. 6 and 11. Input parameters: $k_f = 0.25\ s^{-1}$, $k_r = 0.5\ s^{-1}$, $T_{1PCr} = 3.5$ s, $T_{1\gamma ATP1} = T_{1\gamma ATP2} = 2.5$ s. Neglecting the ATP compartmentalization in the analysis resulted in errors in flux determination and in F_f/F_r.

compartmentalization, an analysis using model I generated errors in the determination of the rate constants, of the forward flux, and of the ratio F_f/F_r, but provided a correct estimation of the reverse CK flux.

Variation of $T_{1\gamma ATP2}$ for a constant fraction f_{ATP}

As shown above, the two-site three-compartment analysis (model II) theoretically allows an estimation of $T_{1\gamma ATP2}$. To test the sensitivity of this determination, $T_{1\gamma ATP2}$ was modified by increasing the viscosity of solution with glycerol, keeping constant the fraction of ATP not involved in CK reaction ($f_{ATP} = 0.45$). Because of increased viscosity, $T_{1\gamma ATP2}$ decreased from 2.5 to 0.8 s, as measured by IR in the absence of CK. The values of $T_{1\gamma ATP2}$ obtained from the inv-γATP protocol were in good correlation ($r^2 = 0.94$, $n = 5$) with those measured by IR.

In conclusion, these in vitro data provided an experimental validation of the theoretical analysis used and showed that the presence of an ATP compartment, f_{ATP}, not involved in the CK reaction disturbed the measured kinetics in IT experiments in a predictable manner. In the case of this simple model, accurate estimation of f_{ATP} was obtained with inv-PCr. In the inv-ATP protocol, a two-site two-compartment analysis correctly measured F_r despite errors in all rate constants. The two-site three-compartment analysis, in addition to leading to a correct estimation of all kinetic parameters, provided an independent estimation of f_{ATP} and a measure of the intrinsic longitudinal relaxation of ATP in the compartment.

Application to the perfused rat heart

Characteristics of the hearts

In the various magnetization protocols hearts developed similar contractile performances; the mean pooled values were LVP = 148 ± 4 mm Hg, frequency = 271 ± 6 beats·min^{-1} and rate pressure product = 4.0 ± 0.1 × 10^4 mmHg · beats·min^{-1} ($n = 24$). No significant rise in end diastolic pressure occurred during the experiment. Metabolite concentrations during the magnetization transfer period were similar for all inversion protocols; the pooled values were ATP = 6.8 ± 0.3 mM, PCr = 12.3 ± 0.3 mM, P_i = 2.9 ± 0.2 mM, pH_i = 7.09 ± 0.01 (PCr to ATP ratio = 1.96 ± 0.09). Creatine was 11.6 ± 0.3 mM and free ADP assuming CK equilibrium was 47 ± 2 μM ($n = 24$).

The parameters of the forward CK flux measured by time-dependent saturation of γATP are shown in Table 2. Forward CK flux was 1.02 ± 0.04 MU·s^{-1} (7.3 ± 0.3 mM·s^{-1}), and T_{1PCr} was 3.2 ± 0.3 s ($n = 4$), in agreement with published data (Stepanov et al., 1997). Indeed, neither ATP compartmentalization nor ATP-P_i exchange should influence the determination of the forward flux parameters by TDST.

Inversion transfer

An inversion PCr protocol is shown in Fig. 2 *a* as well as the time evolution of $M_{\gamma ATP}$ and M_{PCr} in a typical heart (Fig. 2 *b*). The mean k_f and forward CK flux measured by inv-PCr (0.55 ± 0.03 s^{-1} and 1.05 ± 0.06 MU·s^{-1} respectively) were similar to those measured by TDST (Table 2). Notice, however, that k_{1f} was higher (and thus T_{1PCr} was lower) in the inv-PCr protocol. The reverse flux was markedly larger than F_f, and thus the ratio F_f/F_r, 0.51 ± 0.04, was signifi-

TABLE 2 Parameters of the forward and reverse CK flux in perfused hearts: comparison of the protocols of time-dependent saturation transfer of γATP, inversion transfer of PCr, and inversion transfer of γATP analyzed in the two-site two compartment model I

	Saturation γATP ($n = 4$)	Inversion PCr ($n = 5$)	Inversion γATP ($n = 5$)
Parameters of the forward CK flux PCr → ATP			
k_f (s^{-1})	0.58 ± 0.04	0.55 ± 0.03	1.26 ± 0.22*
k_{1f} (s^{-1})	0.91 ± 0.05	1.01 ± 0.04	1.22 ± 0.14
T_{1PCr} (s)	3.15 ± 0.28*	2.22 ± 0.09	
Flux F_f ($MU \cdot s^{-1}$)	1.02 ± 0.04	1.05 ± 0.06	2.31 ± 0.38*
Parameters of the reverse CK flux ATP → PCr			
k_r (s^{-1})		2.16 ± 0.23	1.34 ± 0.07*
k_{1r} (s^{-1})		3.07 ± 0.19	2.97 ± 0.12
$T_{1\gamma ATP1}$ (s)		1.28 ± 0.29	0.62 ± 0.04
Flux F_r ($MU \cdot s^{-1}$)		2.15 ± 0.24	1.26 ± 0.05*
F_f/F_r		0.51 ± 0.04†	1.80 ± 0.25*†

All results are mean ± SE. PCr and ATP (in magnetization units) were the mean values of control spectra (interpulse delay = 10 s) obtained just before and after the inversion transfer. Flux were expressed in magnetization units·s^{-1}. PCr to ATP ratios were similar in inv-PCr and inv-ATP protocols (1.91 ± 0.10 and 1.94 ± 0.07, respectively).
*Comparison with inv-PCr protocol (significant difference $p < 0.05$).
†Significantly different from unity ($p < 0.05$).

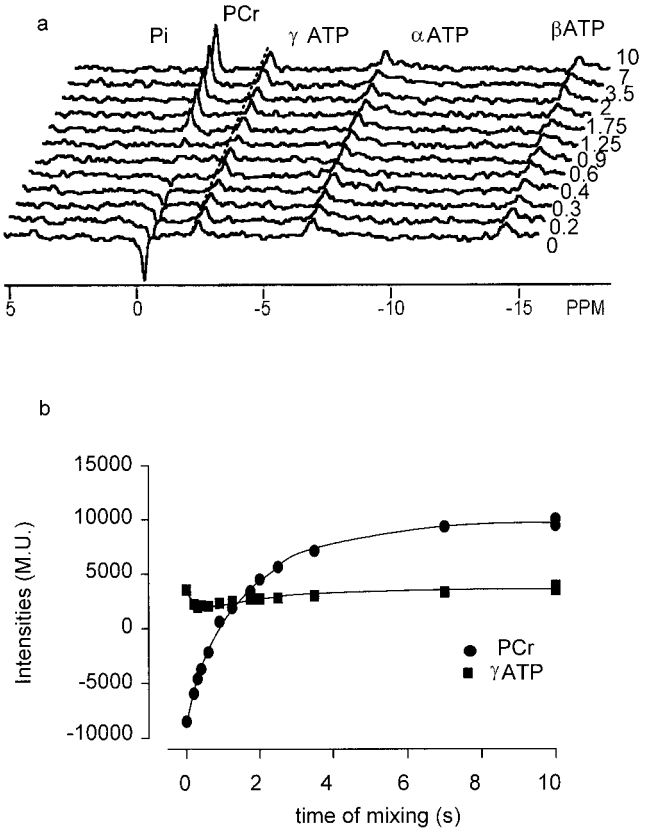

FIGURE 2 Inversion of PCr in a representative heart. (*a*) Stacked plot of the spectra obtained for various times of mixing after the sinc pulse selectively inverting PCr (time of mixing in seconds on the *right*). The dotted line shows the equilibrium magnetization of the noninverted species expected in the absence of inversion. (*b*) Variation of PCr and ATP magnetizations (in magnetization units) as a function of the time of mixing.

cantly lower than unity ($p < 0.001$). According to our in vitro approach, this suggests that 49% of cellular ATP did not participate in the CK reaction.

Fig. 3 shows a typical inv-γATP protocol. When analyzed in model I, the mean F_f appeared to be twice as high as the value determined by TDST or by inv-PCr protocol (Table 2). As a result, F_f/F_r, 1.80 ± 0.25, was significantly different from 1 ($p < 0.01$). Again, by analogy with the in vitro model overestimation of F_f/F_r could result from the presence of an ATP compartment. Table 3 presents the individual analysis in model I of each heart used in the inv-ATP protocol: the parameters of the reverse flux were determined with small confidence intervals (at most 15% on k_r and k_{1r}). Yet the insufficiency of this model was clearly shown by the impossibility of estimating T_{1PCr} (in four of five inv-γATP hearts, k_f was $\geq k_{1f}$).

Hence, by comparison with the in vitro study, the results of both inv-PCr and inv-ATP protocols could be directly explained by the existence of a fraction of ATP that did not exchange with PCr through CK. However, the importance of this fraction and the impossibility of determining T_{1PCr} by inv-γATP suggest that the simple model II was not sufficient to describe myocardial CK flux.

Inversion transfer with saturation of P_i

Elimination of the effect of an ATP-P_i exchange was achieved by continuous saturation of P_i. Sat-P_i decreased the steady-state magnetization of both ATP and PCr (by 15 ± 1 and 14 ± 1%, respectively, $n = 10$) and affected CK kinetic parameters (Table 4).

In inv-PCr, all parameters of the forward CK flux (k_f and F_f), including k_{1f} and T_{1PCr}, were similar, in that protocol, to those measured by saturation of γATP (Table 2). Thus TDST and PCr inversion transfer with saturation of P_i are fully equivalent for the detection of forward flux in myocardium. The ratio F_f/F_r (0.80 ± 0.06) was still significantly different from 1 ($p < 0.05$). According to our in vitro model, this suggests the existence of a 20% ATP compartmentalization.

In inversion of γATP, a complex two-site, three-compartment analysis was required to account for the presence of ATP compartmentalization. Indeed, allowing all parameters to fit without constraints resulted in huge confidence intervals (for instance, ~200% on k_1 determination). However, the mean values of the forward and reverse parameters obtained (data not shown) were not statistically different from those of Table 4, which presents the analysis performed by imposing the forward flux parameters. The observed ratio F_f/F_r (0.67 ± 0.11) still suggests the existence

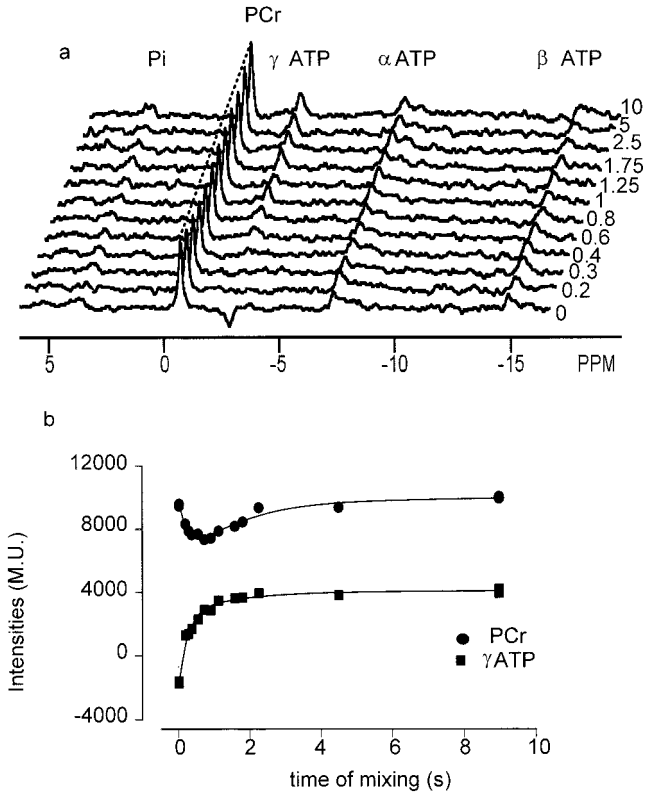

FIGURE 3 Inversion of γATP in a representative heart. Same legend as for Fig. 2. Transfer of magnetization between γ- and βATP could not be demonstrated.

of a significant ATP fraction of 33%. Although this triple compartment analysis of inv-ATP was difficult in the heart, f_{ATP} was similar to that measured by inv-PCr. No significant difference was found in the apparent intrinsic relaxation time of ATP_2 and ATP_1; $T_{1\gamma ATP1}$ was also similar to that measured by inv-PCr protocol. Notice that with saturation of P_i, if the presence of the ATP compartment was neglected (i.e., analysis in model I), the mean F_r value (1.01 ± 0.07 MU·s^{-1}), was similar to F_f obtained in inv-PCr, as also expected from the in vitro study, suggesting the relevance of the compartmentalization model.

Thus, under conditions supposed to mask the effect of the $P_i \rightarrow$ ATP transfer by a continuous saturation of P_i, the two inversion protocols independently revealed the existence of a significant ATP compartment (~20% of myocardial ATP) not involved in the CK reaction.

DISCUSSION

Ability of the different techniques to reveal ATP compartmentalization

As shown in vitro, a complete time analysis of the magnetization recoveries in an IT protocol is able to reveal the existence of an ATP compartment isolated from CK. As expected from the theory, neglecting ATP compartmentalization (i.e., performing the analysis in model I) resulted in an apparent flux discrepancy in both inv-PCr and inv-ATP protocols (an underestimation of F_f/F_r in the former and its overestimation in the latter; Fig. 1). The same behavior was observed in myocardium (Table 2), clearly confirming the insufficiency of the two-site, two-compartment exchange model to account for myocardial energy transfer.

The possibility of detecting an ATP compartment by NMR depends on the type of NMR transfer protocol (Table 1). For instance, when ATP P_i exchange was masked, flux discrepancy could not be evidenced by steady state or time-dependent saturation transfer (Ugurbil et al., 1986; Spencer et al., 1988). As discussed in the Theory section and previously reported (Bittl and Ingwall, 1985), such an ATP compartmentalization cannot be revealed by TDST. Furthermore, its effects will be minimized by an analysis of the initial rates of recovery in an IT or a 2D protocol, as easily demonstrated from the Bloch equations (Meyer et al., 1982; Korestky et al., 1985; DeFuria, 1985). Indeed, no discrepancy between the F_f and F_r has ever been revealed by initial rate analysis in muscle (Hsieh and Balaban, 1988; McFarland et al., 1994).

The results of magnetization transfer experiments are also highly dependent on the experimental conditions (Table 1). For example, in glucose substrate and basal working conditions, equal fluxes were observed by a complete analysis of inversion and by steady-state saturation transfer (Degani et al., 1985). The flux discrepancy, when observed, was suggested to be directly related to the level of cardiac performance (Koretsky et al., 1985); indeed both the ATP-P_i exchange and the amount of ATP present in the mitochondrial matrix (Soboll and Bunger, 1981) are directly related to work. Moreover, most authors, except the group of Ingwall (Bittl and Ingwall, 1985; Bittl et al., 1987; Spencer et al., 1988), observing that the flux discrepancy seen in vivo (Koretsky et al., 1986; Hsieh and Balaban, 1988; Mora et al., 1992) or in hearts using acetate or pyruvate (Nunally and Hollis, 1979; Matthews et al., 1982; Ugurbil et al., 1986; Zweier and Jacobus, 1987) disappeared with glucose utilization (Matthews et al., 1982; Ugurbil et al., 1986; Zweier and Jacobus, 1987), suggested that the contribution of contaminating reactions or ATP compartmentalization was masked by the higher CK flux observed in glucose. Last, various pulse protocols were used in the different studies. Mora et al. (1992), using a long repetition time of 10 s, allowing relaxation of each species, as in our work, could also reveal the apparent flux discrepancy. In contrast, when using a short repetition time of 4 s (similar to T_{1PCr}), like that of Degani et al. (1985), we could no longer find evidence of the flux discrepancy (F_f/F_r was 1.04 in inv-PCr and 1.08 in inv-ATP, $n = 2$). This might suggest that some reaction contributing to the detected flux was eliminated by fast pulsing. Although the exact contributions of the various factors (work, substrate, pulse conditions) are

TABLE 3 γATP inversion transfer experiments in individual rat hearts: analysis in model I (two-site, two-compartment)

Heart	k_r	k_{1r}	$T_{1\gamma ATP}$	k_f	k_{1f}	T_{1PCr}
1	1.58 (0.18)	3.38 (0.31)	0.56	2.08 (0.51)	1.79 (0.29)	−3.45
2	1.36 (0.16)	3.11 (0.32)	0.57	0.99 (0.34)	0.79 (0.17)	−5.00
3	1.14 (0.10)	3.02 (0.21)	0.53	1.51 (0.33)	1.18 (0.16)	−3.03
4	1.22 (0.11)	2.68 (0.21)	0.68	1.11 (0.31)	1.15 (0.17)	
5	1.38 (0.12)	2.68 (0.20)	0.77	0.62 (0.27)	1.17 (0.17)	1.82
Mean	1.34	2.97	0.62	1.26	1.22	−2.42
SE	0.07	0.12	0.04	0.22	0.14	1.28

Parameters are defined in the Theory section. The interval of confidence of the fit is shown in parentheses for each parameter. Variability between hearts is shown by the mean ± SE values. Notice that this analysis allowed the determination of $T_{1\gamma ATP}$ but not of T_{1PCr} (in four of five hearts k_f is equal or superior to k_{1f}).

difficult to appreciate, we believe that they may explain the impossibility of experimentally detecting the presence of an ATP compartment in some previous work.

We further demonstrated that when P_i magnetization was continuously saturated during inversion experiments, the parameters of forward CK flux were similar in protocols of inversion (Table 4) and saturation of γATP (Table 2) and thus can be consistently determined. Absolute flux values (Table 5) were also similar to F_f previously measured by γATP saturation (Koretsky et al., 1986; Ugurbil et al., 1986; Stepanov et al., 1997), in which neither ATP compartmentation nor ATP-P_i exchange induces errors in CK parameters. Although Koretsky et al. (1985) and Brindle (1988) previously suggested that the inversion and the saturation protocols differ in their capacity for CK flux detection, here we show that, when inversion was performed with saturation of P_i, the two techniques were equivalent for the detection of the forward flux. The advantage of the complete analysis of an IT experiment over the other experimental protocols is, however, its ability to quantify ATP compartmentalization by two independent methods (inv-PCr and inv-γATP).

Flux discrepancy observed with saturation of P_i can be understood in the hypothesis of an ATP compartmentalization

The origin of the observed discrepancy of forward and reverse flux has been alternately attributed to the existence

TABLE 4 Comparison of the parameters of forward and reverse CK fluxes measured in the perfused heart by inversion PCr and inversion of γATP under continuous saturation of P_i magnetization

	Inversion PCr ($n = 5$)	Inversion γATP ($n = 5$)	
		Analysis in model I	Analysis in model II
Parameters of the forward CK flux			
k_f (s^{-1})	0.56 ± 0.03	0.78 ± 0.05*	0.57 ± 0.03
k_{1f} (s^{-1})	0.88 ± 0.03	1.00 ± 0.08	0.88 ± 0.03
T_{1PCr} (s)	3.22 ± 0.16	5.4 ± 1.1	3.22 (fixed)
Flux F_f (MU · s^{-1})	0.96 ± 0.12	1.32 ± 0.10	0.96 (fixed)
Parameters of the reverse CK flux			
k_r (s^{-1})	1.36 ± 0.16	1.19 ± 0.08	1.85 ± 0.17*
k_{1r} (s^{-1})	3.39 ± 0.30	2.94 ± 0.12	3.42 ± 0.33
$T_{1\gamma ATP1}$ (s)	0.53 ± 0.06	0.55 ± 0.02	0.70 ± 0.09
Flux F_r (MU · s^{-1})	1.22 ± 0.16	1.01 ± 0.07	1.63 ± 0.23
Analysis			
F_f/F_r	0.80 ± 0.06†	1.32 ± 0.06*†	0.67 ± 0.11†
f_{ATP} (%)	20 ± 6		33 ± 11
$T_{1\gamma ATP2}$ (s)			0.66 ± 0.06

Continuous saturation of P_i decreased the steady-state magnetization of PCr and ATP. This decrease, expressed as a percentage of steady-state magnetization M^∞ (measured in the absence of P_i saturation with a 10-s repetition time), was 14 ± 1% for PCr and 15 ± 1% for γATP ($n = 10$). The PCr to ATP ratio was similar in the two protocols (1.87 ± 0.11 and 2.01 ± 0.14 in inv-PCr and inv-ATP, respectively). The analysis in model II was performed with fixed parameters to improve the interval of confidence of the fit. T_{1PCr} was measured in both protocols of inv-PCr with P_i saturation and TDST. Because inv-PCr and inv-γATP were performed on different hearts, F_f (and not k_f) was fixed to account for any eventual variation in PCr content of the individual hearts.

*Comparison with inv-PCr protocol (significant difference $p < 0.05$).

†F_f/F_r significantly different from unity ($p < 0.05$) (concomitantly f_{ATP} differed from zero) supporting the hypothesis of ATP compartmentalization.

TABLE 5 Summary of flux measurements in myocardium

Type of protocol	n	F_f (mM·s^{-1})	F_r (mM·s^{-1})
Time-dependent saturation of γATP	4	7.3 ± 0.3	
Inversion of PCr	5	7.5 ± 0.4	15.4 ± 1.7*†
Inversion of γATP	5	16.5 ± 2.7*	9.0 ± 0.4†
Inversion of PCr with saturation of P_i	5	6.9 ± 0.8	8.7 ± 1.1‡
Inversion of γATP with saturation of P_i	5	9.5 ± 0.8‡	7.2 ± 0.5‡

*Significant difference between fluxes measured by inversion protocols and F_f measured by TDST ($p < 0.05$, variance analysis and Student-Newman-Keuls).
†Significant difference between forward and reverse flux in each protocol ($p < 0.05$, paired t-test).
‡Influence of P_i saturation, significant difference in the presence and absence of P_i saturation ($p < 0.05$, t-test).

of an ATP compartmentation (model II; Nunnally and Hollis, 1979), the exchange of ATP with species other than PCr (model III; Ugurbil et al., 1986; Spencer et al., 1988), or the influence of a small invisible ATP pool in saturation protocols (Koretsky et al., 1985; Zahler et al., 1987). We do not favor the last as the source of flux discrepancy observed in our inversion protocol. Indeed, in a saturation protocol, the influence of a small invisible ATP pool on the evolution of M_{PCr} could be detected. However, in a pulse labeling technique like ATP inversion, the change in PCr magnetization being proportional to the size of the inverted compartment, such a small invisible ATP pool would have a minimal effect on the exchange, as discussed earlier (Koretsky et al., 1985; Brindle, 1988). Furthermore, this invisible ATP must be small because the ATP content of a normoxic heart is identical when measured by NMR or biochemistry (Humphrey and Garlick, 1991). Thus the exclusive hypothesis of an invisible ATP pool would not be able to account for our inversion data.

The continuous saturation of P_i resonance makes it possible to mask the influence of the ATP-P_i exchange on the measured CK kinetics (Ugurbil et al., 1986). We indeed observed a clear convergence between the data obtained in vitro and those obtained in perfused rat heart with sat-P_i. All data of both inv-ATP and inv-PCr protocols (Table 4) could thus be understood in the hypothesis of an ATP compartment that does not exchange with PCr in model II. This two-site, three-compartment model is a minimal model for cardiac CK explored with saturation of P_i, i.e., a model fitting the data with the smallest number of unknown parameters (two fluxes, one fraction of ATP and T_1s).

How to understand the data obtained without saturation of P_i

Sat-P_i decreased the steady-state magnetization of both PCr and ATP by ~15%, as already observed (Ugurbil et al., 1986). Furthermore, sat-P_i affected kinetic parameters of the forward and reverse CK, as shown by comparison of Tables 4 and 2. Considering the only consequence of sat-P_i to be the masking of $P_i \rightarrow$ ATP exchange, it should be possible to theoretically reconstruct the data of Table 2 simply by adding the influence of this exchange to the experimental results of Table 4. The simulation (shown in the Appendix and Table 6) suggests that experimental data of Table 2 and the decrease in steady-state magnetization induced by P_i saturation were not fully described by the models considered. As already suggested in the analysis of saturation transfer protocol (Brindle, 1988), the mask of $P_i \rightarrow$ ATP exchange per se is not expected to have such an influence on CK flux determination. Moreover, the equivalent decrease in steady-state magnetizations M^{∞}_{PCr} and $M^{\infty}_{\gamma ATP}$ induced by sat-P_i was not anticipated (Table 6). This suggests that sat-P_i might not just eliminate the contribution of the ATP-P_i exchange, but might also affect other cellular reactions or metabolites implying PCr: an exchange between PCr and ATP_2 appears to be a good candidate for contributing to the decreased M^{∞}_{PCr}. In conclusion, model IV should be refined to account for the results observed in the absence of P_i saturation.

Physiological considerations and their expected NMR consequences

The model developed here allowed us to explain both inversion experiments with sat-P_i, suggesting that the system studied by NMR could be mimicked with the minimal simple assumption of an ATP not being involved in the CK reaction. Moreover, this fraction, 20–33% of total cellular ATP, was in the range of mitochondrial ATP content described in the literature for isolated cardiac mitochondria, isolated cardiac myocytes, or hearts performing medium work (Asimakis and Sordall, 1981; Soboll and Bunger, 1981; Geisbuhler et al., 1984). In the hypothesis of ATP_2 localized in the mitochondrial matrix ($ATP_2 = ATP_m$), a more physiological scheme can be proposed. Indeed, we have not considered until now the NMR complexity arising from the specific localization of CK isoforms in myocardium (Nunnally and Hollis, 1979; Koretsky et al., 1985; Zahler et al., 1987), particularly the high proportion of mitochondrial CK (mito-CK ≅ 20% of total CK) localized in the intermembrane space of mitochondria in the vicinity of translocase. Fig. 4, which schematizes the myocardial phosphorus exchanges, includes cytosolic and mitochondrial CK and the restriction of diffusion for CK metabolites, which separates their function.

TABLE 6 Comparison of the change observed with saturation of P_i and the simulation of the effect of the ATP-P_i exchange

	F_f/F_r		Decrease in steady-state magnetization induced by sat-P_i	
	Inv-PCr prot.	Inv-ATP prot.	ATP	PCr
Experimental data: effect of sat_i				
With sat-P_i	0.80 ± 0.06	1.32 ± 0.06	15 ± 1	14 ± 1
Without sat-P_i	0.51 ± 0.04	1.80 ± 0.25		
Computed data: simulation of the influence of the ATP-P_i exchange				
Model III	0.94	1.25	13	8
Model IV	0.79	1.74	26	11
Model IVb	0.81	1.17	19	6

Experimental data: with sat-P_i (data of Table 4), without sat P_i (data of Table 2) (for F_f/F_r $n = 5$; for the decrease in steady-state magnetization, $n = 10$).

Decrease in steady-state magnetization induced by sat-P_i: for ATP = $(M^{\infty}_{ATP} - M^{\infty *}_{ATP})/M^{\infty}_{ATP}$ and for PCr = $(M^{\infty}_{PCr} - M^{\infty *}_{PCr})/M^{\infty}_{PCr}$ with M^{∞} and $M^{\infty *}$ = steady-state magnetization in the absence or presence of P_i saturation, respectively.

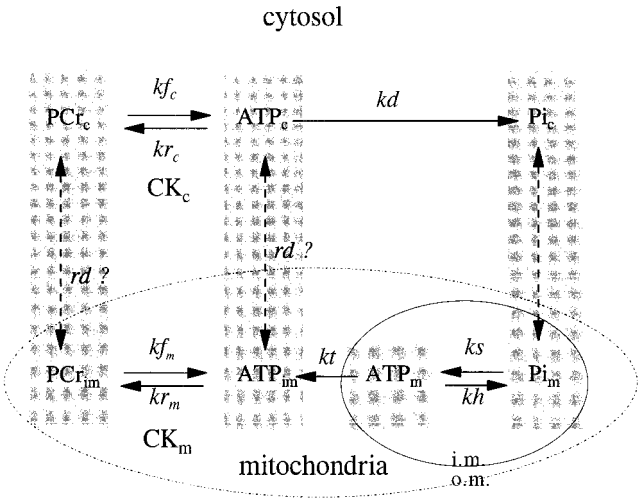

FIGURE 4 Schematic representation of myocardial CK. The model takes into account compartmentalization of mitochondrial CK isoenzyme (CK_m) located in the intermembrane in the vicinity of translocase. CK_c refers to both cytosolic and myofibrillar CK. *Gray areas*, metabolite compartment: P_i, ATP_1, ATP_2 and PCr. Subscript m relates to mitochondrial matrix, c to cytosol, and im to intermembrane space (between the inner and outer mitochondrial membranes). k, rate constants: k_f and k_r, CK flux of ATP and PCr synthesis, respectively. k_t, rate constant of ATP efflux from mitochondrial matrix by adenine nucleotide translocase. The influx of ATP to the matrix was neglected because under high activation of mitochondrial respiration (i.e., when the heart works) the translocase predominantly extrudes ATP from the matrix to the mitochondrial intermembrane space. k_s and k_h, rate constants of mitochondrial ATP synthesis and hydrolysis, respectively. The presence of oxidative substrate (acetate or pyruvate) is well known to inhibit myocardial glycolytic ATP production in normoxia. Thus the $P_i \rightarrow$ ATP reaction can be considered in our experimental design to be restricted to the mitochondrial matrix. k_d, rate of ATP hydrolysis, referring to the cytosolic ATP-P_i flux. The myofibrillar ATPase, responsible for 90% of ATP $\rightarrow P_i$ hydrolysis in the myocardium, is irreversible (thus the reverse cytosolic flux k_d, was neglected). *rd?*, putative restriction of diffusion. ATP exchange with species other than P_i was considered negligible because a transfer of magnetization from γATP to βATP, indicative of a significant adenylate kinase activity, was never observed.

By these hypotheses the time variation of ATP_c under sat-P_i is described by Eq. 4 and that of ATP_m by $dM_{ATP_m}/dt = -(k_t + k_h + 1/T_{1\gamma ATP_m})(M_{\gamma ATP_m} - M^*_{\gamma ATP_m})$. Because ATP_m does not participate in the CK reaction, inv-PCr does not affect this pool. In case of inv-ATP, the return to equilibrium of the ATP_m pool is independent of CK. Thus in terms of NMR, ATP_m will also behave as if it were isolated from the CK reaction, despite the fact that it is in physiological exchange with ATP_c (as shown in Fig. 4). Hence there is no contradiction between isolation of ATP_m by NMR procedure and the fact that up to 90% of cellular ATP is ultimately labeled in a skeletal muscle when net phosphoryl transfer flux is measured by ^{18}O exchange kinetics (Zeleznikar and Goldberg, 1991).

The mitochondrial ATP synthesis and its hydrolysis by myofibrillar, sarcoplasmic reticulum, and sarcolemmal ATPases imply, when translated to an NMR experiment, that sat-P_i would mainly affect mitochondrial metabolites when glycolytic ATP production is negligible (which is the case here because of acetate utilization). Thus mito-CK could be an indirect target of sat-P_i (Fig. 4). In this hypothesis, considering an exchange of $ATP_2 \rightarrow$ PCr through mito-CK flux and metabolite steady state, an equal decrease in M^{∞}_{PCr} and $M^{\infty}_{\gamma ATP}$ could be simulated when the formalism of the Appendix is used. Notice that our results do not exclude the possible existence, however, between ATP_m and PCr, of a small intermediate ATP pool (ATP_{im}) exchanging with CK, which might be the invisible ATP pool previously suggested (Koretsky et al., 1985; Zahler et al., 1987).

Finally, the comparison of data obtained with and without sat-P_i might make it possible to quantify the contribution of mito-CK flux in the whole organ. This hypothesis is currently being tested under various physiological conditions. This also suggests the necessity of considering not only cytosolic CK but also the function of bound enzymes and restrictions of diffusion to fully understand the NMR data. Indeed, the activities of mitochondrial and cytosolic CK (Aliev and Saks, 1997), as well as the consequences of mito-CK activity on flux determined by saturation transfer (Zahler et al., 1987), have already been modeled but still await extensive experimental validation. We believe that our approach of IT analysis has the potential to produce more experimental information on subcellular exchanges.

APPENDIX

Our minimal model of ATP compartmentalization (model II) was fully compatible with the results of the experiments with the saturation of P_i

(Table 4). Thus if saturation of P_i simply masks the P_i-ATP exchange, it must be theoretically possible, knowing the flux of ATP synthesis, to mimic the results of the inversion protocol without saturation of P_i (Table 2).

The rationale was to generate computed data, using the CK parameters obtained with saturation of P_i (Table 4), and to introduce an ATP-P_i exchange estimated from cardiac work. Computed data were then analyzed in a two-site, two-compartment exchange system (model I). Simulation produced evidence of the errors in the F_f/F_r ratio induced by the omission of both ATP-P_i fluxes and the ATP compartment and can be compared with the experimental data of Table 2. Furthermore, we computed the decrease in steady-state magnetization of γATP and PCr expected in each model from a continuous saturation of P_i.

Bloch equations in model IV are described by

$$\frac{\mathrm{d}}{\mathrm{d}t}\begin{pmatrix} M_{\mathrm{PCr}} \\ M_{\gamma\mathrm{ATP1}} \\ M_{\gamma\mathrm{ATP2}} \\ M_{\mathrm{Pi}} \end{pmatrix} = \begin{pmatrix} -k_{1\mathrm{f}} & k_{\mathrm{r}} & 0 & 0 \\ k_{\mathrm{f}} & -k_{1\mathrm{r}} & 0 & k_{\mathrm{d}'} \\ 0 & 0 & -k_{1\mathrm{h}} & k_{\mathrm{s}} \\ 0 & k_{\mathrm{d}} & k_{\mathrm{h}} & -k_{1\mathrm{s}} \end{pmatrix} \cdot \begin{pmatrix} M_{\mathrm{PCr}} - M^{\infty}_{\mathrm{PCr}} \\ M_{\gamma\mathrm{ATP1}} - M^{\infty}_{\gamma\mathrm{ATP1}} \\ M_{\gamma\mathrm{ATP2}} - M^{\infty}_{\gamma\mathrm{ATP2}} \\ M_{\mathrm{Pi}} - M^{\infty}_{\mathrm{Pi}} \end{pmatrix}$$

where

$$k_{1\mathrm{f}} = k_{\mathrm{f}} + \frac{1}{T_{1\mathrm{PCr}}}$$

$$k_{1\mathrm{r}} = k_{\mathrm{r}} + k_{\mathrm{d}} + \frac{1}{T_{1\gamma\mathrm{ATP}}}$$

$$k_{1\mathrm{h}} = k_{\mathrm{h}} + \frac{1}{T_{1\gamma\mathrm{ATP}}}$$

$$k_{1\mathrm{s}} = k_{\mathrm{s}} + k_{\mathrm{d}'} + \frac{1}{T_{1\mathrm{Pi}}}$$

Input parameters

The ATP synthesis rate (2.3 $\mathrm{mM} \cdot \mathrm{s}^{-1}$) was inferred from the work and oxygen consumption (10 μmol/O_2/min/gWW) developed, assuming a P/O ratio of 3, as previously described (Stepanov et al., 1997). The ATP synthesis rate was thus threefold lower than CK flux, in agreement with previous data (Matthews et al., 1982; Koretsky et al., 1986; Stepanov et al., 1997). $T_{1\mathrm{Pi}}$ was taken to be equal to 1 s (from Brindle, 1988). Both $T_{1\gamma\mathrm{ATP1}}$ and $T_{1\gamma\mathrm{ATP2}}$ (considered equals) were calculated from the relation $1/T^{*}_{1\gamma\mathrm{ATP}} = k_{\mathrm{d}} + 1/T_{1\gamma\mathrm{ATP}}$ (see Theory), assuming $k_{\mathrm{d}}\mathrm{ATP}^{\infty}_1$ flux (net utilization) = 1/3 of CK flux: $T_{1\gamma\mathrm{ATP1}} = T_{1\gamma\mathrm{ATP2}} = 0.7$ s. The fraction of f_{ATP} was 0.2 (from Table 4).

The results of the simulation are shown in Table 6 for model IV and for an extension of model IVb that considers the possibility of an additional exchange $\mathrm{ATP}_2 \rightarrow \mathrm{ATP}_1$ (and unidirectional $\mathrm{ATP}_1 \rightarrow P_i$ and $P_i \rightarrow \mathrm{ATP}_2$ fluxes to ensure the steady state of metabolites). To compare to the influence of ATP-P_i exchange in a saturation transfer protocol saturation (Brindle, 1988), we also used model III (although this model was shown to be incompatible with our experimental data with saturation of P_i).

Simulation of the effect of ATP P_i exchange in model IV could mimic the experimental change in F_f/F_r induced by sat-P_i in inv-ATP but not those in inv-PCr (from 0.80 to 0.51); in fact the decrease in F_f/F_r observed in inv-PCr under sat-P_i was expected in none of the models. Furthermore, the equal decline in steady-state magnetization of PCr and ATP observed under sat-P_i could not be simulated; in all models the decrease in $M^{\infty}_{\mathrm{ATP}}$ is expected to be higher than that of $M^{\infty}_{\mathrm{PCr}}$. In conclusion, none of the models tested appeared to be adequate to mimic the totality of the observed effects of sat-P_i (i.e., the results of inv-PCr and of inv-ATP of Table 2 and the steady-state decrease in PCr and ATP magnetization induced by saturation of P_i).

We thank R. Fischmeister for suggesting the in vitro experiments and C. Roby for stimulating discussions. The help of P. Lechene and S. Bigard with the programs of analysis and the manuscript correction by E. Boehm are greatly appreciated.

Part of this work was presented as a communication to the 43rd Meeting of the Biophysical Society (Joubert et al., 1999).

REFERENCES

Aliev, M. K., and V. A. Saks. 1997. Compartmentalized energy transfer in cardiomyocytes: use of mathematical modeling for the analysis of in vivo regulation of respiration. *Biophys. J.* 73:428–445.

Asimakis, G. K., and A. L. Sordahl. 1981. Intramitochondrial adenine nucleotides and energy linked functions of heart mitochondria. *Am. J. Physiol.* 241:H672–H678.

Bittl, J. A., J. Delayre, and J. S. Ingwall. 1987. Rate equation for creatine kinase predicts the in vivo reaction velocity: ^{31}P NMR surface coil studies in brain, heart and skeletal muscle of the living rat. *Biochemistry.* 26:6083–6090.

Bittl, J. A., and J. S. Ingwall. 1985. Reaction rates of creatine kinase and ATP synthesis in the isolated rat heart. A ^{31}P NMR magnetization transfer study. *J. Biol. Chem.* 260:3512–3517.

Brindle, K. M. 1988. NMR methods for measuring enzyme kinetics in vivo. *Prog. NMR Spectrosc.* 20:257–293.

DeFuria, R. R. 1985. Computer simulation of the ^{31}P NMR equations governing the creatine kinase reaction. *J. Theor. Biol.* 114:75–91.

Degani, H., J. R. Alger, R. G. Shulman, O. A. C. Petroff, and J. W. Pritchard. 1987. ^{31}P magnetization transfer studies of creatine kinase kinetics in living rabbit brain. *Mag. Res. Med.* 5:1–12.

Degani, H., M. Laughlin, S. Campbell, and R. G. Shulman. 1985. Kinetics of creatine kinase in heart: a ^{31}P NMR saturation and inversion transfer study. *Biochemistry.* 24:5510–5516.

Geisbuhler, T., R. A. Altschuld, R. W. Trewyn, A. Z. Ansel, K. Lamka, and G. P. Brierley. 1984. Adenine nucleotide metabolism and compartmentalization in isolated adult rat heart cells. *Circ. Res.* 54:536–546.

Hoerter, J. A., C. Lauer, G. Vassort, and M. Guéron. 1988. Sustained function of normoxic hearts depleted in ATP and phosphocreatine: a ^{31}P NMR study. *Am. J. Physiol.* 255:C192–C201.

Hsieh, P. S., and R. S. Balaban. 1988. Saturation and inversion transfer studies of creatine kinase kinetics in rabbit skeletal muscle in vivo. *Mag. Res. Med.* 7:56–64.

Humphrey, S. M., and P. B. Garlick. 1991. NMR-visible ATP and P_i in normoxic and reperfused rat hearts: a quantitative study. *Am. J. Physiol.* 260:H6–H12.

Joubert, F., P. Mateo, B. Gillet, J.-C. Beloeil, and J. A. Hoerter. Myocardial ATP compartmentation evidenced by NMR inversion transfer analysis of creatine kinase fluxes. *Biopjys. J.* 76:A308.

Kingsley-Hickman, P., E. Y. Sako, P. Mohanakrishnan, P. M. L. Robitaille, A. H. L. From, J. E. Foker, and K. Ugurbil. 1987. ^{31}P NMR studies of ATP synthesis and hydrolysis kinetics in the intact myocardium. *Biochemistry.* 26:7501–7510.

Koretsky, A. P., V. J. Basus, T. L. James, M. P. Klein, and M. W. Weiner. 1985. Detection of exchange reactions involving small metabolite pools using NMR magnetization transfer techniques: relevance to subcellular compartmentation of creatine kinase. *Mag. Res. Med.* 2:586–594.

Koretsky, A. P., S. Wang, M. P. Klein, T. L. James, and M. W. Weiner. 1986. ^{31}P NMR saturation measurements of phosphorus exchange reactions in rat heart and kidney in situ. *Biochemistry.* 25:77–84.

Led, J. J., and H. Gesmar. 1982. The applicability of the magnetization transfer technique to determine chemical exchange rates in extreme

cases. The importance of complementary experiment. *J. Mag. Res.* 49:444–463.

Matthews, P. M., J. L. Bland, D. G. Gadian, and G. K. Radda. 1982. A ^{31}P NMR saturation transfer study of the regulation of creatine kinase in the rat heart. *Biochim. Biophys. Acta.* 721:312–320.

McConnell, H. M. 1958. Reaction rates by nuclear magnetization resonance. *J. Chem. Phys.* 28:430–431.

McFarland, E. W., M. J. Kushmerick, and T. S. Moerland. 1994. Activity of creatine kinase in a contracting mammalian muscle of uniform fiber type. *Biophys. J.* 67:1912–1924.

Meyer, R. A., M. J. Kushmerick, and T. R. Brown. 1982. Application of ^{31}P-NMR spectroscopy to the study of striated muscle metabolism. *Am. J. Physiol.* 242:C1–C11.

Mora, B. N., P. T. Narasimhan, and B. D. Ross. 1992. ^{31}P magnetization transfer studies in the monkey brain. *Mag. Res. Med.* 26:100–115.

Nunnally, R. L., and D. P. Hollis. 1979. Adenosine triphosphate compartmentation in living hearts: a phosphorus magnetic resonance saturation transfer study. *Biochemistry.* 18:3642–3646.

Soboll, S., and R. Bunger. 1981. Compartmentation of adenine nucleotides in the isolated working guinea pig heart stimulated by noradrenaline. *Hoppe-Seylers Z. Physiol. Chem.* 362:125–132.

Spencer, R. G., J. A. Balschi, J. S. Leigh, and J. S. Ingwall. 1988. ATP synthesis and degradation rates in the perfused rat heart. ^{31}P nuclear magnetization resonance double saturation transfer measurements. *Biophys. J.* 54:921–929.

Stepanov, V. P., P. Mateo, B. Gillet, J.-C. Beloeil, and J. A. Hoerter. 1997. Kinetics of creatine kinase in an experimental model of low phosphocreatine and ATP in the normoxic heart. *Am. J. Physiol.* 273: C1397–C1408.

Ugurbil, K. 1985. Magnetization-transfer measurements of individual rate constants in the presence of multiple reactions. *J. Mag. Res.* 64:207–219.

Ugurbil, K., M. A. Petein, R. Maiden, S. P. Michurski, and A. H. L. From. 1986. Measurement of an individual rate constant in the presence of multiple exchanges: application to creatine kinase rates. *Biochemistry.* 25:100–108.

Van Dorsten, F. A., M. G. J. Nederhoff, K. Nicolay, and C. J. A. Van Echteld. 1998. ^{31}P NMR studies of creatine kinase flux in M-creatine kinase-deficient mouse heart. *Am. J. Physiol.* 275:1191–1199.

Zahler, R., J. A. Bittl, and J. S. Ingwall. 1987. Analysis of compartment of ATP in skeletal and cardiac muscle using ^{31}P nuclear magnetic resonance saturation transfer. *Biophys. J.* 51:883–893.

Zahler, R., and J. S. Ingwall. 1992. Estimation of heart mitochondrial creatine kinase flux using magnetization transfer NMR spectroscopy. *Am. J. Physiol.* 262:H1022–H1028.

Zeleznikar, R. J., and N. D. Goldberg. 1991. Kinetics and compartmentation of energy metabolism in intact skeletal muscle determined from ^{18}O labeling of metabolite phosphoryls. *J. Biol. Chem.* 266:15110–15119.

Zweier, J. L., and W. E. Jacobus. 1987. Substrate induced alterations of high-energy phosphate metabolism and contractile function in the perfused heart. *J. Biol. Chem.* 262:8015–8021.